Utilizing insulating nanoparticles as the spacer in laminated flexible polymer solar cells for improved mechanical stability

2012 Nanotechnology 23 344007

(http://iopscience.iop.org/0957-4484/23/34/344007)

IOP Publishing Nanotechnology

Nanotechnology **23** (2012) 344007 (6pp) doi:10.1088/0957-4484/23/34/344007

Utilizing insulating nanoparticles as the spacer in laminated flexible polymer solar cells for improved mechanical stability

Yunzhang Lu[1,2,4], Clement Alexander[1,3,4], Zhengguo Xiao[1], Yongbo Yuan[1], Runyu Zhang[1] and Jinsong Huang[1]

[1] Department of Mechanical and Materials Engineering and Nebraska Center for Materials and Nanoscience, University of Nebraska-Lincoln, Lincoln, NE 68588-0656, USA
[2] Key Laboratory of Luminescence and Optical Information, Ministry of Education, Institute of Optoelectronic Technology, Beijing Jiaotong University, Beijing, 100044, People's Republic of China
[3] Department of Chemistry, Emory and Henry College, Emory, VA 24327, USA

E-mail: jhuang2@unl.edu

Received 17 January 2012, in final form 21 March 2012
Published 10 August 2012
Online at stacks.iop.org/Nano/23/344007

Abstract

Roll-to-roll lamination is one promising technique to produce large-area organic electronic devices such as solar cells with a large through output. One challenge in this process is the frequent electric point shorting of the cathode and anode by the excess or concentrated applied stress from many possible sources. In this paper, we report a method to avoid electric point shorting by incorporating insulating and hard barium titanate ($BaTiO_3$) nanoparticles (NPs) into the active layer to work as a spacer. It has been demonstrated that the incorporated $BaTiO_3$ NPs in poly(3-hexylthiophene):[6,6]-phenyl-C-61-butyric acid methyl ester (P3HT:PCBM) bulk heterojunction solar cells cause no deleterious effect to the power conversion process of this type of solar cell. The resulting laminated devices with NPs in the active layer display the same efficiency as the devices without NPs, while the laminated devices with NPs can sustain a ten times higher lamination stress of over 6 MPa. The flexible polymer solar cell device with incorporated NPs shows a much smaller survivable curvature radius of 4 mm, while a regular flexible device can only sustain a bending curvature radius of 8 mm before fracture.

(Some figures may appear in colour only in the online journal)

1. Introduction

The polymer solar cell (PSC) is a promising new type of photovoltaic device with the advantages of easy fabrication, flexibility, light weight, large-area and low cost production using convenient thin film deposition technology; it also has considerable potential in renewable energy resources [1–3]. Bulk heterojunction (BHJ) based PSCs have an active layer consisting of conjugated polymer donor and soluble fullerene derivative acceptor. Recently, power conversion efficiencies (PCEs) of 8%–10% for the new donor or new acceptor materials BHJ solar cells have been reported which brings PSCs closer to the market [4–8]. For massive production of PSCs, it is desirable to fabricate PSCs by a fast and economical process with high-throughput, such as the continuous roll-to-roll manufacturing process [9–11]. The lamination fabrication process is one possible technique for fulfilling these requirements [12, 13]. This process has been previously used by us and other groups to form a transparent electrode made of indium tin oxide (ITO) [12], semitransparent Ag nanowire [14] and graphene [15] for polymer solar cells which avoids the step of high vacuum metal deposition for metallization. Furthermore, a Ag electrode on a flexible PEN substrate has been used in laminated poly(3-hexylthiophene) (P3HT):[6, 6]-phenyl-C-61-butyric acid methyl ester (PCBM) solar cells with a PCE

[4] Y Lu and C Alexander contributed to this work equally.

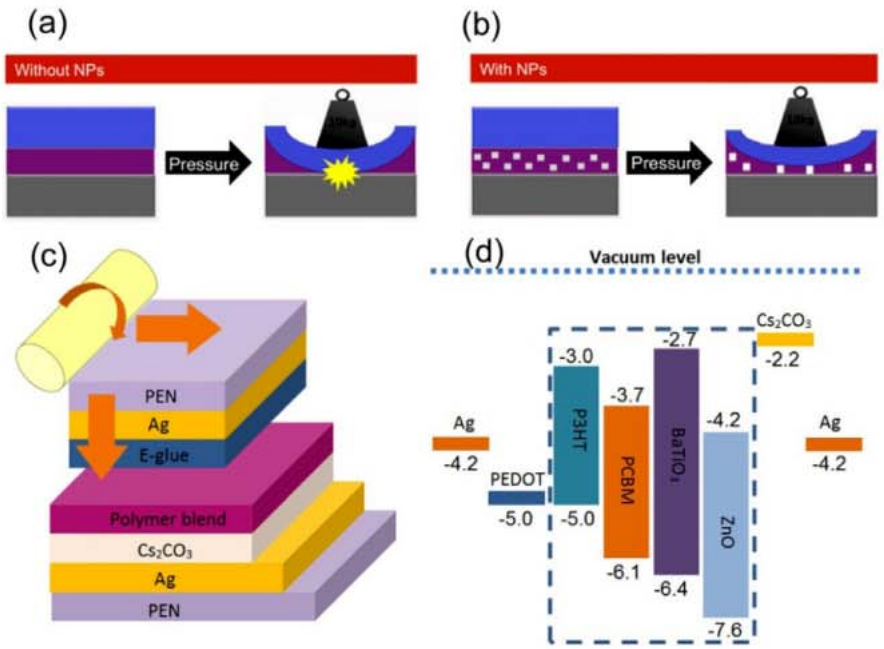

Figure 1. (a), (b) The illustration of the formation of a laminated polymer solar cell with and without incorporation of NPs as a spacer. Concentrated stress can deform the soft active layer causing the shorting of cathode and anode, and the incorporated hard NPs can prevent the shorting of cathode and anode; (c) the device structure and lamination process to form the polymer solar cells; (d) diagram of the energy level of the materials used in this study.

up to 4.0% [16]. Despite all of this promising progress, there is still one critical issue in the roll-to-roll lamination process which might dim its advantages: how to form both good electronic contact and mechanical contact at the polymer/electrode interface for high PCE as well as for good mechanical stability and high durability. One possible problem with fabricating devices by lamination is the formation of electric short points caused by concentrated stress. The electric shorting points form because the polymer active layer is relatively soft and concentrated stress on the flexible electrodes generates spikes or protuberances on the electrodes creating a direct electric contact between them [17]. This problem is magnified in all-flexible PSC devices because frequent bending of the flexible device inevitably generates cracks which are also sources of short points.

In this study, the insulating barium titanate ($BaTiO_3$) nanoparticles (NPs) were introduced into the active layer of the PSCs as spacers for a high yield lamination process. The concept is illustrated in figures 1(a) and (b). Acting as a spacer between the two electrodes, the hard $BaTiO_3$ NPs, with a Young's modulus much higher than that of the soft polymer active layer, helps to maintain the integrity of the active layer, and enhances the yield of device fabrication by lamination.

In order to maintain efficiency of PSCs with incorporated NPs, the selection of NPs should follow a few guidelines: (1) the NPs need to have good insulation properties so that they will not shorten the two electrodes by themselves; (2) the NP material should have a high Young's modulus so that it can sustain a much higher stress than the polymer; (3) the NP material should have appropriate energy levels so that they will not act as a charge trapper; (4) the NP material should be cost effective so as not to add much cost to the manufacturing process. In this work, $BaTiO_3$ was chosen as the spacer material fulfilling all these requirements. For example, $BaTiO_3$ has high elastic modulus beyond 100 GPa which is ten times that of P3HT or PCBM [18, 19]. It is also a good insulator with high relative permittivity of 2500 [20]. Due to the low conduction band bottom of -2.7 eV and high ionization energy of -6.4 eV [21], $BaTiO_3$ NPs will not trap electrons or holes from PCBM or P3HT.

2. Experimental details

2.1. Material preparation

For the photoactive materials, P3HT and PCBM were selected as donor and acceptor, respectively [22–24]. Regioregularity P3HT and PCBM were purchased from Rieke Metals, Inc. and Nano Carbon Inc. respectively. Poly(3,4-ethylenedioxythiophene):poly(styrenesulfonate) (PEDOT:PSS, Clevios PH 1000) was purchased from H C Starck, Inc. 1,2-dichlorobenzene (DCB) was purchased from Sigma-Aldrich. Polyethylene naphthalate (PEN, Teonex Q65F) was purchased from DuPont Teijin Films. Cubic $BaTiO_3$ NPs (average size of 50 nm) was purchased from Advanced Materials, Inc. All these materials were used as received without further treatment.

To prepare the blend P3HT:PCBM solution with NPs, the $BaTiO_3$ NPs were dispersed in DCB with a concentration of 1 mg ml^{-1}. After several days' sedimentation, excess aggregated $BaTiO_3$ NPs formed a white precipitate at the bottom of the solution. NPs in the top layer appeared well dispersed in a clear solution. This top layer of solution was

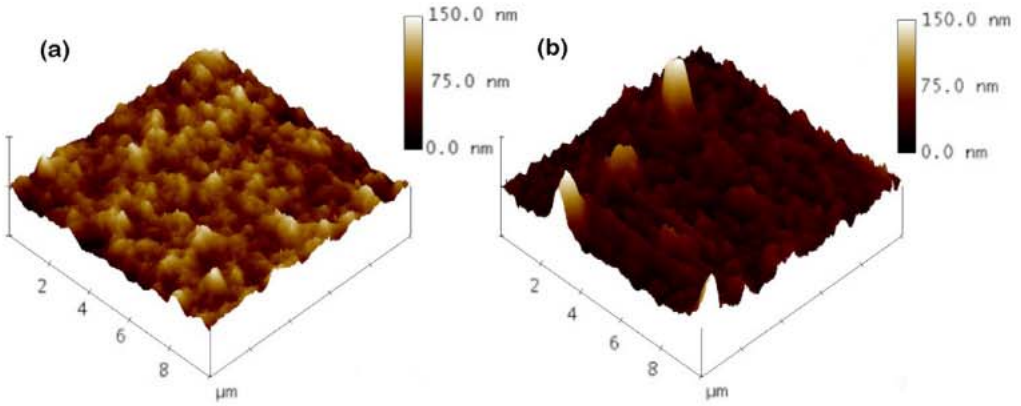

Figure 2. Surface morphology of active layer incorporated with/without NPs. AFM height images with a 10 μm × 10 μm surface area: (a) without NPs; (b) with NPs.

filtered with a 0.45 μm filter in order to remove largely conglomerated NPs. After filtering, the $BaTiO_3$ solution with a concentration of 0.2 mg ml^{-1} was mixed with P3HT and PCBM at a concentration of 17 mg ml^{-1} each. To fabricate control devices without NPs, P3HT and PCBM (1:1 by wt) were dissolved in DCB to make a 34 mg ml^{-1} solution. Both blend solutions were stirred overnight at 40 °C in a glove box to fully dissolve them.

In the $BaTiO_3$ NPs solution mentioned above, the weight ratio of $BaTiO_3$ NPs and P3HT:PCBM was 1:170. The average surface density of $BaTiO_3$ NPs is estimated to be 2 μm^{-2}.

2.2. Device fabrication

To fabricate the devices, the ITO substrates first underwent a routine cleaning procedure, which consisted of repeated rinsing in deionized water, ultrasonic processing in acetone and isopropyl alcohol, and final treatment with ultraviolet (UV) ozone. The PEN substrates were cleaned by First Contact Polymer (Photonic Cleaning Technologies). After cleaning, a buffer layer of cesium carbonate (Cs_2CO_3) was spin-coated onto the ITO/glass substrate at a spin speed of 4000 rpm to form a cathode, which corresponded to a thickness of 1–3 nm, and baked at 150 °C for 10 min. Then the active layer was prepared by spin-coating the polymer blend at 800 rpm for 20 s, which underwent a slow drying process in a covered glass petri dish. The thickness of the film was about 200 nm. Before the lamination process, the films were thermally annealed at 110 °C for 10 min. On the anode side, a 100 nm thick Ag layer was deposited on the PEN substrate by thermal evaporation. The adhesive and conductive layer (referred to as E-glue) was obtained by doping D-sorbitol into PEDOT:PSS, which was spin-coated on the Ag layer to form an adhesive anode. After drying both substrates, they were laminated together by a moderate pressure tightly gluing them together. The device structure and lamination process are illustrated in figures 1(c) and (d). The details of the lamination process are described in previous reports [16]. In order to study the stability of devices with all-flexible substrates, both the anode and cathode utilized PEN as substrate and Ag as electrode. The fabrication steps of making an all-flexible device are the same as those mentioned above.

2.3. Measurement

The current–voltage characteristics of the devices were measured under simulated AM 1.5G irradiation (100 mW cm^{-2}) using a xenon-lamp-based solar simulator (Oriel 96000 150 W solar simulator). Atomic force microscopy (AFM) images were measured by Digital Instruments Nanoscope III (Veeco Instruments Inc.) under tapping mode.

3. Results and discussions

3.1. Surface morphology of active layer with/without NPs as the spacer in laminated PSCs

The AFM images for surface morphology of the active layer are shown in figure 2. As seen in figure 2(a), the surface of polymer layer is relatively rough for the samples without $BaTiO_3$ NPs because a slow drying process was used for the P3HT:PCBM film [3]. The surface roughness σ of the active layer is 5.3 nm. For samples with NPs, a rough surface with σ ∼ 23.8 nm was measured. The existence of convex topography can be easily observed, as the bright spots shown in figure 2(b). It is noted the size and height of the bumps in the AFM picture are a little bigger than the individual $BaTiO_3$ NP size. One possible explanation is that $BaTiO_3$ NPs aggregate into small dots in the polymer. The degree of aggregation can be estimated from the bump density on the P3HT:PCBM surface which is around one NP μm^{-2}. Therefore each bump on average contains about two NPs.

3.2. Effect of the NPs in lamination devices under pressure and bending

To determine if the addition of NPs can improve the mechanical resistance to externally applied stress and the effect of NPs on the performance of devices, we first fabricated glass/ITO substrate PSC devices by lamination

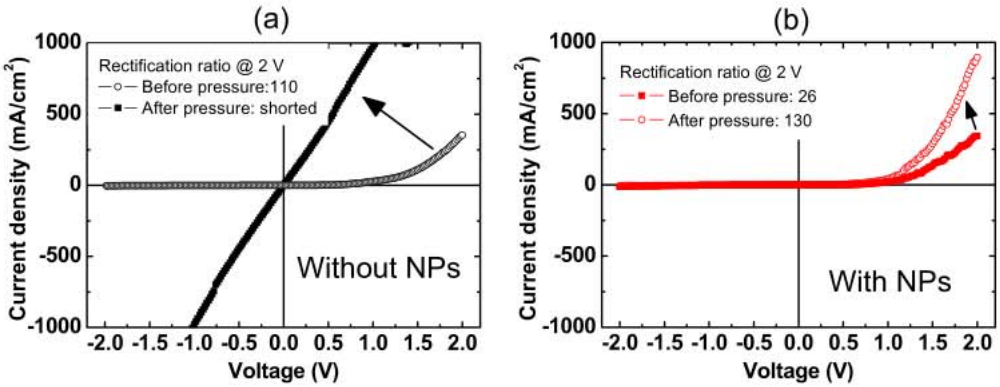

Figure 3. Comparison of the dark I–V curves of devices before and after 6.0 MPa of pressure was applied to the working area of the glass/ITO substrate device. (a) Without NPs; device shorted after pressure was applied. (b) With NPs; device remained working after pressure was applied.

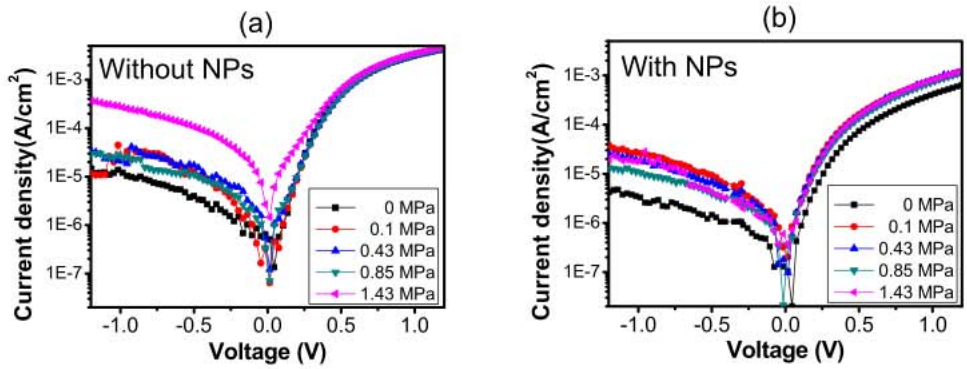

Figure 4. The dark I–V curves of all-flexible substrate devices with and without NPs were tested under various pressures: (a) without NPs; (b) with NPs.

using polymer solution with and without $BaTiO_3$ NPs. The dark I–V curves of these devices were measured and are shown in figure 3. By applying 6.0 MPa pressure on the working area of each device, the device without NPs in the active layer had an obvious electric point short form, while the device with NPs had a good resistance to mechanical stress and even got a better device performance. These results can probably be explained by the soft polymer active layer easily piercing under the concentrated pressure due to its low Young's modulus, leading to a direct contact between the two electrodes in the absence of NP spacers. After incorporating high Young's modulus NPs in the device, robust active layer/electrode contact was maintained and an enlarged device working area was obtained due to the external pressure. For these reasons, the chance of electric point shorts occurring under elevated stress will be significantly reduced in devices utilizing NPs.

Flexible PSCs need to have both substrates flexible. Here we used Ag/PEN as both sides of the device to demonstrate the function of the $BaTiO_3$ spacer in preventing point contacts in the lamination process. For this experiment, the structure of the device used Ag/Cs_2CO_3/active layer/PEDOT:PSS/Ag. It is not a working solar cell device because both sides have opaque Ag electrodes with a thickness of 100 nm. Only the dark I–V curve of the device was measured under various pressures.

The dark I–V curves of all-flexible devices were measured under a series of applied pressures from 0 to 1.43 MPa, and the results are shown in figure 4. As seen in figure 4(a), for devices without NPs the reverse bias dark current suddenly increases by more than ten times after a critical applied stress of 1.43 MPa which indicates the formation of a short point. The I–V curves of the device with NPs did not show the abrupt changing despite a slight change under the wide range of applied mechanical stresses, as shown in figure 4(b). The small increase of current (both forward and reverse biased) could be explained by the increased contact area during the lamination due to the possible presence of large $BaTiO_3$ NPs aggregating in the film. This result clearly proves the function of $BaTiO_3$ NPs in preventing the formation of point short contacts in the flexible solar cell device.

The effect of the incorporated NPs on the mechanical property of all-flexible polymer solar cell devices was also tested. Again the variation of dark current was measured to evaluate the quality of the device under different bending conditions. Figure 5(a) is the side view of the device during bending testing. The bending angles were calculated from the curvature of the bending devices. Figure 5(b) shows the evolution of dark current density at a reverse bias of −4 V with the bending angles. For the device without NPs, the dark current suddenly increased when the bending angle is beyond

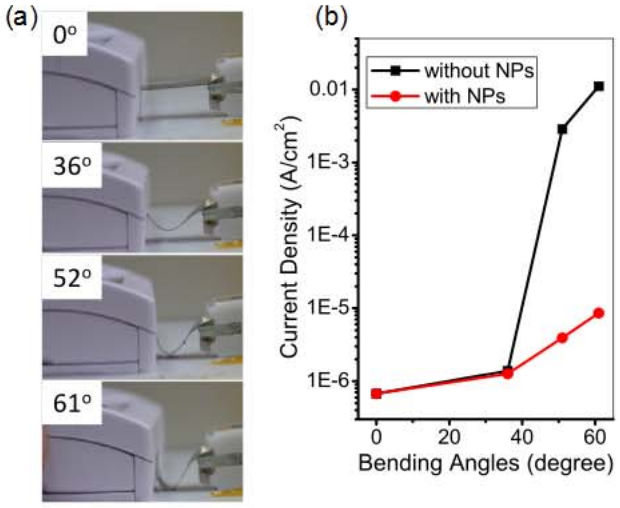

Figure 5. (a) The side view of the bending test of the flexible device. (b) The evolution of dark current at −0.4 V with the bending angles.

35°, which indicates the damage to the polymer active film in the device by the bending process. The corresponding fracture curvature radius is calculated to be 8 mm according to the size of our devices. The dark current of the device with NPs did not show such abrupt increase of dark current until the bending angle exceeded 60°, despite a slight change of dark current which was also observed over a large range of bending angles. The smallest bending radius of the device with NPs reaches 4 mm which is among the smallest reported bending radius for flexible solar cells. This result confirms the function of $BaTiO_3$ NPs in preventing the formation of point short contacts in the flexible solar cell device.

3.3. Efficiency of the laminated devices with/without NPs

It is important that the incorporation of the spacer NPs does not change the device efficiency. To verify this, the photocurrents of the two laminated PSC devices with and without the incorporated NPs were compared, as shown in figure 6(a). Both devices have the structure of ITO/Cs_2CO_3/active layer/PEDOT:PSS/Ag. The device with NPs contained a concentration of 0.2 mg ml^{-1} of $BaTiO_3$ in its photoactive polymer layer. These two devices displayed similar photocurrents. The laminated device without NPs had a short circuit current density (J_{sc}) of 11.4 mA cm^2, an open circuit voltage (V_{oc}) of 0.525 V, a fill factor (FF) of 63.7% and a PCE of 3.81%, which is comparable to our best reported result [16]. The device with NPs had a J_{sc} of 11.1 mA cm^2, a V_{oc} of 0.581 V, a FF of 58.8% and a PCE of 3.79%. Since the PCEs of these two devices were so close it appears that the NPs had no detrimental effect on the conductivity of the photoactive polymer layer.

As a comparison, the incorporation of a zinc oxide (ZnO) NP spacer was chosen for fabricating a PSC. The I–V curves of the device were measured as shown in figure 6(b). Here the device only had a J_{sc} of 0.81 mA cm^{-2}, a V_{oc} of 0.2 V, a FF of 23.7% and a PCE of 0.004%. The poor performance of the device is related to the incorporation of ZnO NPs. As shown in figure 1(d), the conduction band of ZnO is −4.2 eV, while the LUMO of PCBM is −3.7 eV. Therefore ZnO NPs can easily capture electrons from the PCBM by the formation of traps, which greatly reduces the efficiency of the device. Thus the selection of materials with proper energy levels is important, and $BaTiO_3$ satisfies this requirement as shown by experiments performed in this work.

4. Conclusions

In conclusion, these series of experiments have successfully demonstrated the progress of the flexible substrate laminated BHJ solar cells, with an active layer of P3HT:PCBM mixed with $BaTiO_3$ NPs. The introduction of NPs into the active layer increased the mechanical stability under mechanical stress. The device with the added NPs exhibited a PCE of 3.79% under AM 1.5G irradiation, while the device without NPs had a PCE of 3.81%. Since this change in performance is quite small, $BaTiO_3$ did not appear to have a detrimental effect on the conductivity of the active layer. For the all-flexible substrate PSCs, the device containing the NPs endured higher pressures and larger bending angles and the device performance did not change, while the device without NPs

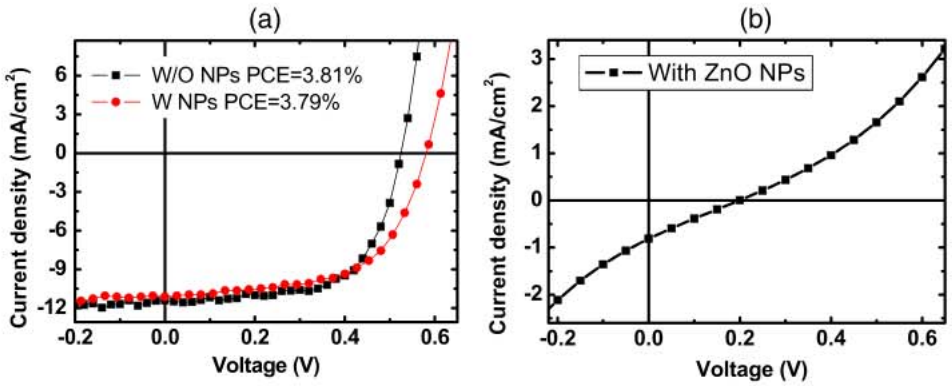

Figure 6. Comparison of the I–V curves of devices (a) without, with $BaTiO_3$ NPs and (b) with ZnO NPs.

developed significant leakage current under certain pressure and bending. This indicates that the NPs can effectively protect the device from damage under stress and thus the mechanical stability of the device can be improved by this method.

Acknowledgments

J Huang acknowledges partial support of this work by the Defense Threat Reduction Agency, Basic Research Award No. HDTRA1-10-1-0098 and the Nebraska Center for Energy Science Research.

References

[1] Carsten D and Vladimir D 2010 Polymer–fullerene bulk heterojunction solar cells **Rep. Prog. Phys. 73** 096401

[2] Kim J Y, Lee K, Coates N E, Moses D, Nguyen T-Q, Dante M and Heeger A J 2007 Efficient tandem polymer solar cells fabricated by all-solution processing **Science 317** 222–5

[3] Li G, Shrotriya V, Huang J, Yao Y, Moriarty T, Emery K and Yang Y 2005 High-efficiency solution processable polymer photovoltaic cells by self-organization of polymer blends **Nature Mater. 4** 864–8

[4] Yuan Y, Reece T J, Sharma P, Poddar S, Ducharme S, Gruverman A, Yang Y and Huang J 2011 Efficiency enhancement in organic solar cells with ferroelectric polymers **Nat. Mater. 10** 296–302

[5] Liang Y, Xu Z, Xia J, Tsai S-T, Wu Y, Li G, Ray C and Yu L 2010 For the bright future—bulk heterojunction polymer solar cells with power conversion efficiency of 7.4% **Adv. Mater. 22** E135–8

[6] Chen H-Y, Hou J, Zhang S, Liang Y, Yang G, Yang Y, Yu L, Wu Y and Li G 2009 Polymer solar cells with enhanced open-circuit voltage and efficiency **Nature Photon. 3** 649–53

[7] Steirer K X **et al** 2011 Enhanced efficiency in plastic solar cells via energy matched solution processed NiO_x interlayers **Adv. Energy Mater. 1** 813–20

[8] Zhao G, He Y and Li Y 2010 6.5% Efficiency of polymer solar cells based on poly (3-hexylthiophene) and indene-C60 bisadduct by device optimization **Adv. Mater. 22** 4355–8

[9] Dupont S R, Oliver M, Krebs F C and Dauskardt R H 2012 Interlayer adhesion in roll-to-roll processed flexible inverted polymer solar cells **Sol. Energy Mater. Sol Cells 97** 171–5

[10] Krebs F C 2009 Polymer solar cell modules prepared using roll-to-roll methods: knife-over-edge coating, slot-die coating and screen printing **Sol. Energy Mater. Sol Cells 93** 465–75

[11] Krebs F C 2009 All solution roll-to-roll processed polymer solar cells free from indium–tin-oxide and vacuum coating steps **Org. Electron. 10** 761–8

[12] Huang J, Li G and Yang Y 2008 A Semi-transparent plastic solar cell fabricated by a lamination process **Adv. Mater. 20** 415–9

[13] Granstrom M, Petritsch K, Arias A C, Lux A, Andersson M R and Friend R H 1998 Laminated fabrication of polymeric photovoltaic diodes **Nature 395** 257–60

[14] Gaynor W, Lee J-Y and Peumans P 2009 Fully solution-processed inverted polymer solar cells with laminated nanowire electrodes **ACS Nano 4** 30–4

[15] Lee Y-Y, Tu K-H, Yu C-C, Li S-S, Hwang J-Y, Lin C-C, Chen K-H, Chen L-C, Chen H-L and Chen C-W 2011 Top laminated graphene electrode in a semitransparent polymer solar cell by simultaneous thermal annealing/releasing method **ACS Nano 5** 6564–70

[16] Yuan Y, Bi Y and Huang J 2011 Achieving high efficiency laminated polymer solar cell with interfacial modified metallic electrode and pressure induced crystallization **Appl. Phys. Lett. 98** 063306

[17] Krebs F C, Jørgensen M, Norrman K, Hagemann O, Alstrup J, Nielsen T D, Fyenbo J, Larsen K and Kristensen J 2009 A complete process for production of flexible large area polymer solar cells entirely using screen printing—first public demonstration **Sol. Energy Mater. Sol. Cells 93** 422–41

[18] Jaglinski T, Kochmann D, Stone D and Lakes R S 2007 Composite materials with viscoelastic stiffness greater than diamond **Science 315** 620–2

[19] Tahk D, Lee H H and Khang D-Y 2009 Elastic moduli of organic electronic materials by the buckling method **Macromolecules 42** 7079–83

[20] Kim P, Jones S C, Hotchkiss P J, Haddock J N, Kippelen B, Marder S R and Perry J W 2007 Phosphonic acid-modified barium titanate polymer nanocomposites with high permittivity and dielectric strength **Adv. Mater. 19** 1001–5

[21] Pontes F, Pinheiro C, Longo E, Leite E, De Lazaro S, Magnani R, Pizani P, Boschi T and Lanciotti F 2003 Theoretical and experimental study on the photoluminescence in $BaTiO_3$ amorphous thin films prepared by the chemical route **J. Lumin. 104** 175–86

[22] Ma W, Yang C, Gong X, Lee K and Heeger A 2005 Thermally stable, efficient polymer solar cells with nanoscale control of the interpenetrating network morphology **Adv. Funct. Mater. 15** 1617–22

[23] Sivula K, Luscombe C K, Thompson B C and Fréchet J M J 2006 Enhancing the thermal stability of polythiophene: fullerene solar cells by decreasing effective polymer regioregularity **J. Am. Chem. Soc. 128** 13988–9

[24] Chen D, Liu F, Wang C, Nakahara A and Russell T P 2011 Bulk heterojunction photovoltaic active layers via bilayer interdiffusion **Nano Lett. 11** 2071–8